Charles Darwin University

Saturation of Open-Circuit Voltage at Higher Light Intensity Caused by Interfacial Defects and Nonradiative Recombination Losses in Perovskite Solar Cells

Ompong, David; Singh, Jai; Sreedhar Ram, Kiran; Setsoafia, Daniel Dodzi Yao; Mehdizadeh Rad, Hooman

Published in:
Advanced Materials Interfaces

DOI:
10.1002/admi.202201578
10.1002/admi.202201578

Published: 05/01/2023

Document Version
E-pub ahead of print

Link to publication

Citation for published version (APA):
Ompong, D., Singh, J., Sreedhar Ram, K., Setsoafia, D. D. Y., & Mehdizadeh Rad, H. (2023). Saturation of Open-Circuit Voltage at Higher Light Intensity Caused by Interfacial Defects and Nonradiative Recombination Losses in Perovskite Solar Cells. *Advanced Materials Interfaces*, *10*(1), 1-5. [2201578]. https://doi.org/10.1002/admi.202201578, https://doi.org/10.1002/admi.202201578

General rights
Copyright and moral rights for the publications made accessible in the public portal are retained by the authors and/or other copyright owners and it is a condition of accessing publications that users recognise and abide by the legal requirements associated with these rights.

- Users may download and print one copy of any publication from the public portal for the purpose of private study or research.
- You may not further distribute the material or use it for any profit-making activity or commercial gain
- You may freely distribute the URL identifying the publication in the public portal

Take down policy
If you believe that this document breaches copyright please contact us providing details, and we will remove access to the work immediately and investigate your claim.

Download date: 05. Oct. 2023

ADVANCED MATERIALS INTERFACES
www.advmatinterfaces.de

Check for updates

Saturation of Open-Circuit Voltage at Higher Light Intensity Caused by Interfacial Defects and Nonradiative Recombination Losses in Perovskite Solar Cells

*David Ompong, Kiran Sreedhar Ram, Daniel Dodzi Yao Setsoafia, Hooman Mehdizadeh Rad, and Jai Singh**

A new analytical expression that directly relates the open-circuit voltage (V_{oc}) in perovskite solar cells (PSCs) to the quasi-Fermi level splitting (QFLS), interface energy offsets, and nonradiative recombination losses has been derived. It is found that the QFLS of the active layer plays a dominant role in enhancing V_{oc} of PSCs. The newly derived V_{oc} is applied to two PSCs with the hole transport layer (HTL) of poly[bis(4-phenyl)(2,4,6-trimethylphenyl)amine], and poly(3-hexylthiophene-2,5-diyl) (P3HT) and found that the first PSC has a higher V_{oc}, which agrees well with the experimental results. It is found that both PSCs exhibit saturation of V_{oc} at the higher charge carrier generation rates and hence at higher light intensities. The lower V_{oc} in PSC with P3HT as HTL is attributed to the stronger band bending and higher interfacial defects. In accordance with the results, a large quasi-Fermi level splitting and a minimal interfacial energy offsets may be considered when selecting material for high V_{oc} PSCs.

1. Introduction

All solar cells have radiative recombination losses which cannot be avoided, however, the additional voltage losses via nonradiative recombination through surfaces and interfaces may be minimized or eliminated.[1–4] Measurements of photoluminescence quantum yield (PLQY) provide a link between V_{oc} and the quasi-Fermi level splitting (QFLS) in perovskite solar cells (PSCs). QFLS is usually obtained from the measurements of PLQY whiles V_{oc} of a device is measured directly.[1–6]

The measurement of V_{oc} as function of light intensity reveals that the V_{oc} increases first, then gets saturated at high illumination intensities (>1 sun)[6,7] and in some solar cells eventually starts to decease; a phenomenon commonly known as back bending.[7] The saturation and back bending of V_{oc} restrict the use of PSCs in concentrated sun applications. Various proposals have been put forward to explain such influence of light intensity on V_{oc} including the increased surface recombination at higher light intensity,[6,8] lower hole bulk conductivity, nonohmic back contacts,[7] and reduced charge separation in the case of built-in potential limited solar cells.[3] Also, a diode model, where the solar cell is considered as the primary diode with an opposing parasitic back contact has been used to explain the saturation of V_{oc}.[7] However, the diode model does not take into account other factors that contribute to V_{oc} saturation, such as low bulk conductivity, bulk and interface defects, and charge carrier mobility imbalance.[7] A minimal energy offset at the perovskite/HTL interface in PSCs facilitates hole transport in maintaining the photogenerated current at any given sun intensity as well as reducing V_{oc} saturation.[6–10] The saturation in V_{oc} occurs due to a saturation in charge carrier extraction in PSCs and back bending occurs due to the build-up of charge carriers with inefficient extraction at the electrodes at very high light intensities, leading to reduction in V_{oc}; similar to the reduction in V_{oc} at larger absorber layer thickness.[5,8] In addition, the presence of energy offset at the perovskite/HTL interface and other nonradiative additional recombination sources can also deplete the charge carriers,[11] which may have a much larger effect on the V_{oc}.[8]

Some analytical V_{oc} expressions derived as a function of temperature in PSCs are well known in the literature.[5,6,12] Using the drift-diffusion model, we have also derived V_{oc} in PSCs as a function of temperature in our earlier work.[13] However, to the best of our knowledge, an expression of V_{oc} as a function of QFLS in PSCs that combines the influence of energy offset at the interfaces and nonradiative recombination has not yet been reported. Therefore, following our previous work,[13] in this paper, we have used the drift-diffusion model by incorporating the additional energy losses at the contacts and derived an expression for the V_{oc} in PSCs as a function of QFLS and nonradiative recombination losses. We then demonstrate that the new V_{oc} thus obtained depends directly on QFLS and PLQY of a PSC. This paper is organized as follows: presented Section 1 presents an introduction, in Section 2 we show the derivation of the V_{oc} using the drift-diffusion model

D. Ompong, K. S. Ram, D. D. Y. Setsoafia, H. Mehdizadeh Rad, J. Singh
College of Engineering, IT and Environment
Charles Darwin University
Darwin, Northern Territory 0909, Australia
E-mail: jai.singh@cdu.edu.au

D. Ompong, H. Mehdizadeh Rad, J. Singh
Energy and Resources Institute
Charles Darwin University
Darwin, Northern Territory 0909, Australia

The ORCID identification number(s) for the author(s) of this article can be found under https://doi.org/10.1002/admi.202201578.

© 2022 The Authors. Advanced Materials Interfaces published by Wiley-VCH GmbH. This is an open access article under the terms of the Creative Commons Attribution License, which permits use, distribution and reproduction in any medium, provided the original work is properly cited.

DOI: 10.1002/admi.202201578

© 2022 The Authors. Advanced Materials Interfaces published by Wiley-VCH GmbH

21967350, 0, Downloaded from https://onlinelibrary.wiley.com/doi/10.1002/admi.202201578 by Charles Darwin University Library, Wiley Online Library on [21/10/2022]. See the Terms and Conditions (https://onlinelibrary.wiley.com/terms-and-conditions) on Wiley Online Library for rules of use; OA articles are governed by the applicable Creative Commons License

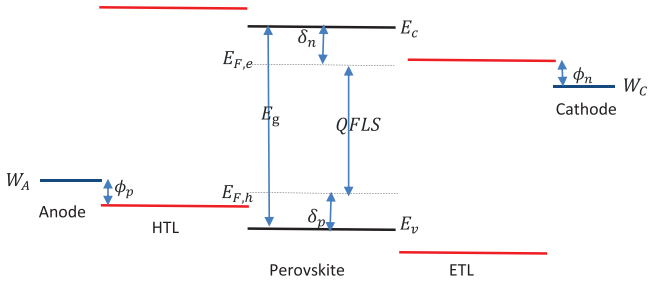

Figure 1. Schematic diagram of the energy levels and interfacial energy offsets in the PSCs.

which depends on QFLS and losses at the contacts of a PSC, the results and discussion about the factors contributing to V_{oc} losses are described in Section 3and Section 4 presents conclusions.

2. Derivation of V_{oc} in PSCs

The V_{oc} in PSCs, is usually defined as[1,12,14]

$$qV_{oc} = E_g - \phi_n - \delta_n - \phi_p - \delta_p \tag{1}$$

where q is the charge of an electron. Using the energy diagram shown in **Figure 1** $\delta_n = E_c - E_{F,e}$, $\delta_p = E_{F,h} - E_v$, $\phi_n = E_{LUMO}^{ETL} - W_C$, $\phi_p = W_A - E_{HOMO}^{HTL}$, and $E_g = E_c - E_v$. It may be noted that the V_{oc} defined in Equation (1) is independent of temperature.

For deriving a V_{oc} as a function of temperature, following our earlier work,[13] we have used the drift-diffusion model, where the total current density J is given as[13,15]

$$J = J_n + J_p = \mu_e n \nabla E_{F,e} + \mu_h p \nabla E_{F,h} \tag{2}$$

where $J_n = \mu_e\ n\nabla E_{F,e}$ is the electron current density and $J_p = \mu_h\ p\nabla E_{F,h}$ is the hole current density, $n(p)$ is the electron (hole) concentration, $\mu_e(\mu_h)$ is the electron (hole) mobility, and $\nabla E_{F,e}(\nabla E_{F,h})$ is the gradient of the electron (hole) quasi-Fermi level. The total current density J in Equation (2) can be expressed in terms of V_{oc} as[13,16]

$$\begin{aligned} J = {} & \mu_e N_c \nabla E_{F,e} \exp\left[\left(qV_{oc} - E_g + \phi_n + \phi_p + \delta_p\right)/k_B T\right] \\ & + \mu_h N_v \nabla E_{F,h} \exp\left[\left(qV_{oc} - E_g + \phi_n + \phi_p + \delta_n\right)/k_B T\right] \end{aligned} \tag{3}$$

As shown in the Appendix, by optimizing J in Equation (3) with respect to V_{oc}, we get

$$qV_{oc} = \mathrm{QFLS} + \Delta E_1 + \Delta E_2 - \phi_n - \phi_p - \delta_n - \Delta V_{oc,NR} \tag{4}$$

where $\Delta E_1 = (E_{F,h} - E_{HOMO}^{HTL}), \Delta E_2 = (E_{HOMO}^{HTL} - E_v)$, $\Delta V_{oc,NR} = k_B T \ln\left(\frac{\mu_h N_v \nabla E_{F,h}}{\mu_e N_c \nabla E_{F,e}}\right)$, and QFLS = $E_{F,e} - E_{F,h}$. Here $E_{F,e}$ and $E_{F,h}$ are the quasi-Fermi levels of electrons and holes, respectively. Although the V_{oc} in Equation (4) depends explicitly on QFLS, it does not exhibit any dependence on the nonradiative recombination.[17] This is because it is assumed in Equation (4) that all nonradiative recombination losses in the perovskite layer and the at interfaces are accounted for by $\Delta V_{oc,NR}$. This assumption is based on the fact that experimentally the nonradiative losses are determined by the photoluminescence quantum yield (PLQY,[1,4,5] which is related with $\Delta V_{oc,NR}$ as[18,19]

$$\Delta V_{oc,NR} = -\frac{k_B T}{q} \ln(\mathrm{PLQY}) \tag{5}$$

The V_{oc} obtained in Equation (4) does not reveal any apparent dependence on the light intensity, which directly affects the generation rate of free charge carriers. In order to show that the V_{oc} in Equation (4), does depend on the generation rate of free charge carriers, we first modified the expression of $\Delta V_{oc,NR}$ as

$$\Delta V_{oc,NR} = k_B T \ln\left(\frac{\mu_h N_v \nabla E_{F,h}}{\mu_e N_c \nabla E_{F,e}}\right) = k_B T \ln\left(\frac{n J_p N_v}{p J_n N_c}\right) = k_B T \ln\left(\frac{n I_p N_v}{p I_n N_c}\right) \tag{6}$$

where I_p and I_n are the hole and electron surface recombination currents,[20] respectively. Then δ_n and I_n are expressed as a function of the rate of charge carrier generation G as[14,20]

$$\delta_n = \frac{k_B T}{2} \ln\left(\frac{\beta N_c^2}{G}\right) + \frac{k_B T}{2} \ln\left(\frac{n}{p}\right) \tag{7}$$

and

$$I_n = qGL_n^* \tag{8}$$

where $G = G_L + \beta n_i^2$, β is the bimolecular recombination coefficient, n_i is the intrinsic carrier concentration and $L_n^* = \left(\frac{2k_B T}{q}\sqrt{\frac{\mu_e \mu_h}{\beta G_L}}\right)^{1/2}$, is the effective diffusion length of electrons. Using Equations (7) and (8) in Equation (4), we get

$$\begin{aligned} qV_{oc} = {} & \mathrm{QFLS} + \Delta E_1 + \Delta E_2 + 2E_g + k_B T \ln\left(\frac{P_{cat}}{N_v}\frac{N_{an}}{N_c}\right) \\ & - \frac{k_B T}{2} \ln\left(\frac{\beta N_c^2}{G}\right) - k_B T \ln\left(\frac{v_{d,p} P_{cat}\left(e^{qV/k_B T} - 1\right)}{G_L L_n^*\left(1 + \frac{v_{d,p}}{S_p}\right)}\right) \end{aligned} \tag{9}$$

where $\phi_n = -E_g - k_B T \ln(P_{cat} N_v)$, $\phi_p = -E_g - k_B T \ln(N_{an} N_c)$, $I_p = \frac{q v_{d,p} P_{cat}(e^{qV/k_B T} - 1)}{(1 + \frac{v_{d,p}}{S_p})}$, and $v_{d,p} = \frac{\mu_h E}{\frac{k_B T}{qEd}(e^{\frac{qEd}{k_B T}} - 1)}$, effective diffusion velocity of holes in the active layer.[14,20]

Here $P_{cat}(N_{an})$ is the equilibrium hole (electron) density at the cathode (anode), $N_c(N_v)$ is the concentration of electrons (holes) at the band edge of the perovskite conduction (valence) band, d is active layer thickness, S_p is hole surface recombination velocity, and E is electric field. Here, we have assumed that the concentrations of electrons (n) and holes (p) are equal and a spatially constant, $G = G_L$, photogeneration rate of free charge carriers.

© 2022 The Authors. Advanced Materials Interfaces published by Wiley-VCH GmbH

21967350, 0, Downloaded from https://onlinelibrary.wiley.com/doi/10.1002/admi.202201578 by Charles Darwin University Library, Wiley Online Library on [21/10/2022]. See the Terms and Conditions (https://onlinelibrary.wiley.com/terms-and-conditions) on Wiley Online Library for rules of use; OA articles are governed by the applicable Creative Commons License

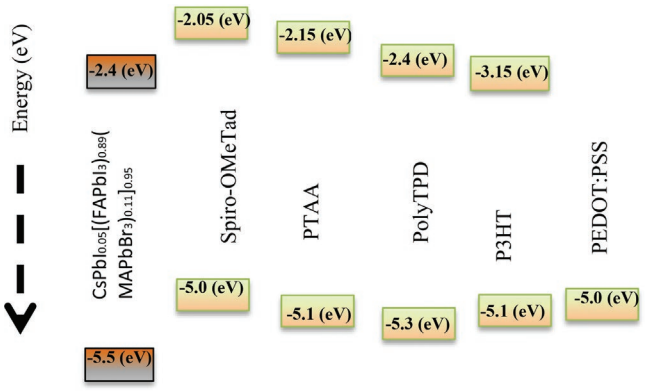

Figure 2. Energy level diagram of the HOMO and LUMO of a perovskite material.[4] and HTL materials[1] used in Table 1.

The last term of V_{oc} derived in Equation (9) is the contribution from the nonradiative recombination of charge carriers in PSCs. In Section 3, the results of both Equations (4) and (9) are presented and discussed.

3. Results and Discussions

For an ideal solar cell one should have $q\ V_{oc}$ = QFLS, which means in Equation (4), $\Delta E_1 = \Delta E_2 = \phi_n = \phi_p = \delta_n = 0$, and $\mu_e N_c \nabla\ E_{F,e} = \mu_h\ N_v \nabla E_{F,h}$.[6,8] The V_{oc} for a real PSC is given by Equation (4), which is used here to calculate the V_{oc} for a perovskite layer forming an interface with different HTLs. The energy level diagram of a perovskite material and the HTL materials are shown in **Figure 2**. These hole transport materials and calculated corresponding V_{oc} from Equation (4) are listed in **Table 1**, along with their experimental values. In this calculation, we have used $\phi_n = \phi_p = 0.1$ eV,[6] $E_v = -5.5$ eV[1] and assumed $E_{F,h} = -5.3$ eV and $\delta_n = 0.1$ eV for all the hole transport materials. We have used the HOMO level of the perovskite layer for the interfacial compatibilizer PFN-P2 at the PFN-P2/perovskite interface in Table 1. Furthermore, the experimental values of QFLS and PLQY as listed in Table 1 are used in the calculation and $\Delta V_{oc,NR}$ is calculated from Equation (5). The V_{oc} thus calculated and listed in Table 1 is therefore intensity independent.

Table 2. Input parameters used for plotting Figure 3, the electron and hole densities are considered equal.

Parameter	PTAA	P3HT	Refs.
S_p [cm s^{-1}]	100	1000	[6]
d [nm]	400	400	[6]
$N_c = N_v = N$ [cm^{-3}]	10×10^{25}	10×10^{25}	[20]
$\mu_h = \mu_e = \mu$ cm^2 V^{-1} s^{-1}]	10	10	[6]
E_g [eV]	1.60	1.60	[6]
QFLS [eV]	1.16	1.07	[6]
P_{cat} [cm^{-3}]	5.1×10^6	2.4×10^8	
ΔE_1 [eV]	0.20	0.20	[1,4]
ΔE_2 [eV]	0.40	0.40	[1,4]
β [cm^3 s^{-1}]	5.17×10^{-12}	5.17×10^{-12}	[20]
E [V μ^{-1} m^{-1}]	6.0×10^{-4}	9.9×10^{-4}	
V [V]	1.75	2.11	
n_i [cm^{-3}]	3.1×10^9	1×10^{10}	

According to Equation (4) and the calculated values in Table 1, as $V_{oc} \approx$ QFLS, the contributions of other terms in Equation (4) to V_{oc} can be regarded to be small. The calculated V_{oc} is found to be in good agreement with the corresponding experimental value for all the materials (see Table 1).

In order to understand the intensity dependence, we have used the input parameters given in **Table 2** in Equation (9) and plotted V_{oc} as a function of the generation rate G_L for two PSCs with different HTLs of PTAA and P3HT in **Figure 3**. Accordingly, the open-circuit voltage of both PSCs increases initially and then gets saturated at higher G_L and such dependence agrees very well with the experimental results (see Figure 3). It may also be noted that V_{oc} of the PSC with HTL of PTAA is found to be about 0.2 V higher than that of the PSC with HTL of P3HT at all G_L and this trend also agrees very well with experimental results.[6] The PSC with HTL of PTAA has also been found to have higher power conversion efficiency than that with P3HT, which is attributed to the higher V_{oc} and this also agrees very well with the experimental result.[6] The lower V_{oc} in the PSC with HTL of P3HT, may be attributed to the relatively higher band bending and interface defects caused by

Table 1. Calculated V_{oc} from Equation (4) for the selected HTL materials, using $\phi_n = \phi_p = \delta_n = 0.1$ eV, $E_{F,h} = -5.3$ eV, and $E_v = -5.5$ eV. The experimental values of QFLS and PLQY are used in the calculation and the experimental values V_{oc}^{expt} are also listed for comparison.

Film/Interface	QFLS [eV]	PLQY [%]	E_{HOMO}^{HTL} [eV]	$\Delta V_{oc,NR}$ [V]	V_{oc}^{calc} [V]	V_{oc}^{expt} [V]
Perovskite	1.208[4]	0.5020[4]	−5.50[1]	0.018	1.10	1.22[4]
PFN-P2/Perovskite	1.206[4]	0.3250[4]	−5.50[1]	0.029	1.08	1.14[4]
PTAA/Perovskite	1.164[6]	0.0261[4]	−5.10[4]	0.095	0.99	1.14[6]
PEDOT:PSS/Perovskite	1.092[1]	0.0075[1]	−5.00[1]	0.127	0.87	0.91[1]
P3HT/Perovskite	1.106[6]	0.0770[1]	−5.10[1]	0.067	0.94	0.95[6]
Spiro-MeTAD/Perovskite	1.172[1]	0.1400[1]	−5.00[1]	0.051	1.02	1.02[1]
PTAA:PFN/Perovskite	1.204[1]	0.5100[1]	−5.10[4]	0.018	1.08	1.14[1]
PolyTPD:PFN/Perovskite	1.208[1]	0.7300[1]	−5.30[1]	0.008	1.10	1.13[1]

© 2022 The Authors. Advanced Materials Interfaces published by Wiley-VCH GmbH

21967350, 0, Downloaded from https://onlinelibrary.wiley.com/doi/10.1002/admi.202201578 by Charles Darwin University Library, Wiley Online Library on [21/10/2022]. See the Terms and Conditions (https://onlinelibrary.wiley.com/terms-and-conditions) on Wiley Online Library for rules of use; OA articles are governed by the applicable Creative Commons License

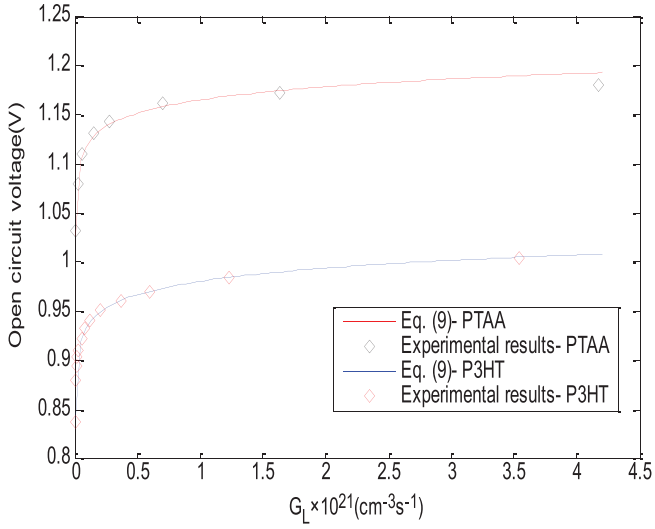

Figure 3. Open-circuit voltage calculate using Equation (9) and input parameters from Table 2 is plotted for two PSCs with HTL of PTAA and P3HT as a function of the generation rate G_L.The corresponding experimental results[6] are also plotted for comparison.

higher E, V, n_i, and P_{cat} as can be seen in Table 2. Thus, the higher electric field in the PSC with HTL of P3HT is needed in order to maintain the current flow at a given light intensity.[7] The relatively higher band bending and interface defects may explain the significant V_{oc} saturation found in the PSC with HTL of P3HT at higher light intensity.[6]

4. Conclusion

We have derived a new analytical expression for V_{oc} in PSCs as a function of the quasi-Fermi level splitting (QFLS), interface energy offsets, and nonradiative recombination losses. It is found that the QFLS plays the dominant role in determining the V_{oc}, although reducing nonradiative recombination and the energy offset at the interfaces can also enhance the V_{oc} in PSCs. Therefore, in accordance with our results, a large quasi-Fermi level splitting and a minimal interfacial energy offsets may be considered when selecting material for high V_{oc} PSCs. We have found that the open-circuit voltage PSCs increases initially and then gets saturated at higher G_L and hence at higher light intensity, which agrees very well with the experimental results. The relatively lower V_{oc} found in PSC with P3HT as HTL is attributed to the stronger band bending and higher interfacial defects. Our results may be expected to be useful in material selection and design of perovskite solar cells.

Appendix: Derivation of Analytical Open-Circuit Voltage

$$E_{F,e} - E_c = -\delta_n = qV_{oc} - E_g + \phi_n + \phi_p + \delta_p \tag{A1}$$

$$E_v - E_{F,h} = -\delta_p = qV_{oc} - E_g + \phi_n + \phi_p + \delta_n \tag{A2}$$

The total current density J can be expressed in terms of V_{oc}

$$\begin{aligned} J(V_{oc}) &= \mu_e N_c \nabla E_{F,e} \exp\left[\left(E_{F,e} - E_c\right)/k_B T\right] \\ &\quad + \mu_h N_v \nabla E_{F,h} \exp\left[\left(E_v - E_{F,h}\right)/k_B T\right] \\ &= \mu_e N_c \nabla E_{F,e} \exp\left[\left(qV_{oc} - E_g + \phi_n + \phi_p + \delta_p\right)/k_B T\right] \\ &\quad + \mu_h N_v \nabla E_{F,h} \exp\left[\left(qV_{oc} - E_g + \phi_n + \phi_p + \delta_n\right)/k_B T\right] \end{aligned} \tag{A3}$$

Optimizing J with respect to V

$$\frac{d}{dV_{oc}}\left[J(V_{oc})\right] = 0 \tag{A4}$$

We obtain

$$\begin{aligned} &\frac{q}{k_B T}\mu_e N_c \nabla E_{F,e} \exp\left[\left(qV_{oc} - E_g + \phi_n + \phi_p + \delta_p\right)/k_B T\right] \\ &\quad + \frac{q}{k_B T}\mu_h N_v \nabla E_{F,h} \exp\left[\left(qV_{oc} - E_g + \phi_n + \phi_p + \delta_n\right)/k_B T\right] \end{aligned} \tag{A5}$$

$$\begin{aligned} &\mu_e N_c \nabla E_{F,e} \exp\left[\left(qV_{oc} - E_g + \phi_n + \phi_p + \delta_p\right)/k_B T\right] \\ &\quad = \mu_h N_v \nabla E_{F,h} \exp\left[\left(qV_{oc} - E_g + \phi_n + \phi_p + \delta_n\right)/k_B T\right] \end{aligned} \tag{A6}$$

$$\mu_e N_c \nabla E_{F,e} \exp\left[\left(\delta_p\right)/k_B T\right] = \mu_h N_v \nabla E_{F,h} \exp\left[\left(\delta_n\right)/k_B T\right] \tag{A7}$$

$$\delta_n - \delta_p = k_B T \ln\left(\frac{\mu_e N_c \nabla E_{F,e}}{\mu_h N_v \nabla E_{F,h}}\right) \tag{A8}$$

Rearranging Equation (1) in the text in the form $-\delta_p - \delta_n = qV_{oc} - E_g + \phi_n + \phi_p$, and in addition to using $\delta_p + \delta_n = E_g - \mathrm{QFLS}$ (see Figure 1) in Equation (A8), we obtained

$$qV_{oc} = \mathrm{QFLS} + \Delta E_1 + \Delta E_2 - \phi_n - \phi_p - \delta_n - k_B T \ln\left(\frac{\mu_h N_v \nabla E_{F,h}}{\mu_e N_c \nabla E_{F,e}}\right) \tag{A9}$$

Rearranging Equation (A9), using Equations (6)–(8) in the text gives

$$\begin{aligned} qV_{oc} &= \mathrm{QFLS} + \Delta E_1 + \Delta E_2 + 2E_g + k_B T \ln\left(\frac{P_{cat}}{N_v}\frac{N_{an}}{N_c}\right) \\ &\quad - \frac{k_B T}{2}\ln\left(\frac{\beta N_c^2}{G}\right) - k_B T \ln\left(\frac{v_{d,p} P_{cat}\left(e^{qV/k_B T} - 1\right)}{G_L L_n^*\left(1 + \frac{v_{d,p}}{S_p}\right)}\right) \end{aligned} \tag{A10}$$

Acknowledgements

Open access publishing facilitated by Charles Darwin University, as part of the Wiley - Charles Darwin University agreement via the Council of Australian University Librarians.

Conflict of Interest

The authors declare no conflict of interest.

© 2022 The Authors. Advanced Materials Interfaces published by Wiley-VCH GmbH

21967350, 0, Downloaded from https://onlinelibrary.wiley.com/doi/10.1002/admi.202201578 by Charles Darwin University Library, Wiley Online Library on [21/10/2022]. See the Terms and Conditions (https://onlinelibrary.wiley.com/terms-and-conditions) on Wiley Online Library for rules of use; OA articles are governed by the applicable Creative Commons License

Data Availability Statement

The data that support the findings of this study are available from the corresponding author upon reasonable request.

Keywords

interfaces, nonradiative recombination, open-circuit voltage saturation, perovskite solar cells, quasi-Fermi level splitting

Received: July 18, 2022
Revised: September 8, 2022
Published online:

[1] M. Stolterfoht, P. Caprioglio, C. M. Wolff, J. A. Márquez, J. Nordmann, S. Zhang, D. Rothhardt, U. Hörmann, Y. Amir, A. Redinger, L. Kegelmann, F. Zu, S. Albrecht, N. Koch, T. Kirchartz, M. Saliba, T. Unold, D. Neher, *Energy Environ. Sci.* **2019**, *12*, 2778.
[2] F. Ebadi, B. Yang, Y. Kim, R. Mohammadpour, N. Taghavinia, A. Hagfeldt, W. Tress, *J. Mater. Chem. A* **2021**, *9*, 13967.
[3] W. Tress, M. Yavari, K. Domanski, P. Yadav, B. Niesen, J. P. Correa Baena, A. Hagfeldt, M. Graetzel, *Energy Environ. Sci.* **2018**, *11*, 151.
[4] M. Stolterfoht, C. M. Wolff, J. A. Márquez, S. Zhang, C. J. Hages, D. Rothhardt, S. Albrecht, P. L. Burn, P. Meredith, T. Unold, D. Neher, *Nat. Energy* **2018**, *3*, 847.
[5] M. Rai, L. H. Wong, L. Etgar, *J. Phys. Chem. Lett.* **2020**, *11*, 8189.
[6] P. Caprioglio, M. Stolterfoht, C. M. Wolff, T. Unold, B. Rech, S. Albrecht, D. Neher, *Adv. Energy Mater.* **2019**, *9*, 1901631.
[7] O. Gunawan, T. Gokmen, D. B. Mitzi, *J. Appl. Phys.* **2014**, *116*, 084504.
[8] D. Głowienka, D. Zhang, F. Di Giacomo, M. Najafi, S. Veenstra, J. Szmytkowski, Y. Galagan, *Nano Energy* **2020**, *67*, 104186.
[9] H. D. Pham, T. T. Do, J. Kim, C. Charbonneau, S. Manzhos, K. Feron, W. C. Tsoi, J. R. Durrant, S. M. Jain, P. Sonar, *Adv. Energy Mater.* **2018**, *8*, 1703007.
[10] N. Arora, S. Orlandi, M. I. Dar, S. Aghazada, G. Jacopin, M. Cavazzini, E. Mosconi, P. Gratia, F. De Angelis, G. Pozzi, M. Graetzel, M. K. Nazeeruddin, *ACS Energy Lett.* **2016**, *1*, 107.
[11] H. Mehdizadeh-Rad, J. Singh, *Materials* **2019**, *12*, 2727.
[12] W. Yang, Y. Yao, C.-Q. Wu, *J. Appl. Phys.* **2015**, *117*, 095502.
[13] D. Ompong, J. Singh, *Org. Electron.* **2018**, *63*, 104.
[14] O. J. Sandberg, M. Nyman, R. Österbacka, *Phys. Rev. Appl.* **2014**, *1*, 024003.
[15] J. Nelson, *The Physics of Solar Cells*, Imperial College Press, London **2003**, p. 363.
[16] D. Ompong, J. Singh, *Front. Nanosci. Nanotechnol.* **2016**, *2*, 43.
[17] Y. Ding, B. Ding, H. Kanda, O. J. Usiobo, T. Gallet, Z. Yang, Y. Liu, H. Huang, J. Sheng, C. Liu, Y. Yang, V. I. E. Queloz, X. Zhang, J.-N. Audinot, A. Redinger, W. Dang, E. Mosconic, W. Luo, F. De Angelis, M. Wang, P. Dörflinger, M. Armer, V. Schmid, R. Wang, K. G. Brooks, J. Wu, V. Dyakonov, G. Yang, S. Dai, P. J. Dyson, *Nat. Nanotechnol.* **2022**, *17*, 598.
[18] S. M. Menke, N. A. Ran, G. C. Bazan, R. H. Friend, *Joule* **2018**, *2*, 25.
[19] R. T. Ross, *J. Chem. Phys.* **1967**, *46*, 4590.
[20] O. J. Sandberg, A. Sundqvist, M. Nyman, R. Österbacka, *Phys. Rev. Appl.* **2016**, *5*, 044005.

© 2022 The Authors. Advanced Materials Interfaces published by Wiley-VCH GmbH

21967350, 0, Downloaded from https://onlinelibrary.wiley.com/doi/10.1002/admi.202201578 by Charles Darwin University Library, Wiley Online Library on [21/10/2022]. See the Terms and Conditions (https://onlinelibrary.wiley.com/terms-and-conditions) on Wiley Online Library for rules of use; OA articles are governed by the applicable Creative Commons License